Determining the superfluid density of superconductors by modeling a Josephson STM as an electrical circuit

Ven, João Maurits van der

Determining the superfluid density of superconductors by modeling a Josephson STM as an electrical circuit

Thesis

submitted in partial fulfillment of the
requirements for the degree of

Bachelor of Science
in
Physics and Astronomy

Author :	João Maurits Marie van der Ven
Student ID :	2057263
Supervisor :	Dr. M.P. Allan, A. Mozes
Second corrector :	Prof.dr. C.W.M. Fridlund

Leiden, The Netherlands, February 15, 2022

Determining the superfluid density of superconductors by modeling a Josephson STM as an electrical circuit

João Maurits Marie van der Ven

Huygens-Kamerlingh Onnes Laboratory, Leiden University
P.O. Box 9500, 2300 RA Leiden, The Netherlands

February 15, 2022

Abstract

In this thesis we look at the frequency dependent properties of a scanning tunneling Microscope (STM) where both the tip and the sample are superconductors. In that case, the tip-sample system is considered an ultra-small Josephson junction. The junction has been modelled as an electrical circuit consisting of a capacitive component C, a kinetic inductive component L_k as well as a Josephson inductive component L_J, also called 'the LC-ciruit model'. Furthermore, the order of magnitude of the parameters have been estimated. We found values for C ranging between $\sim 10^{-13} - 10^{-17}$F, L_k between $\sim 10^{-13} - 10^{-9}$H and L_J around $\sim 10^{-8} - 10^{-7}$H. Finally, we simulated the LC-circuit and found that measuring the resonance frequency ω_c might be a way to determine the superfluid density n of superconductors.

Contents

Chapter 1

Introduction

One of the aims of the Allan Lab at the Leiden Institute of physics is to understand superconductors and explore their properties. An important physical quantity of a superconductor and the protagonist of this research, is the superfluid density n. With which we mean the number of Cooper pairs per unit volume. n is interesting because it tells a lot about a superconductor. The quantity occurs in many equations that relate properties of a superconductor and so can for instance, be used to determine other physical quantities and vice-versa. To measure and 'look' our group makes use of self-build STM's. And that is were the story starts. By bringing a sharp conducting tip close to a conducting sample, and applying a bias voltage a current will start to flow. When we make the tip and the sample of superconductors, we may regard the system as an ultra-small Josephson junction. A range of different effects and equations now describe our system, some containing the superfluid densities of the tip and the sample, n_t and n_s, respectively. Specifically this research aims to understand the frequency dependent properties of the Josephson-STM (J-STM). We modeled our system as an electrical circuit and found that it has a measurable resonance frequency that relates the parameters of the electrical circuit, which represent physical quantities. As some parameters depend upon n_t and n_s, measuring this resonance indirectly means determining n_t and n_s. We present the model, the parameters, what values they take on for an J-STM and how we deduce n_t and n_s from the resonance frequency.

In chapter 2 we explain theory and other important foreknowledge. We will explain what an STM is, what superconductors are, what a Josephson junction is and describe some of the resulting effects. In chapter 3 we will lay the foundation which the rest of the research was build upon. We will present the relevant frequency dependent physical quantities in a J-STM and show how these depend on the superfluid densities of the tip and the sample. In chapter 4 we will present the

LC-circuit model, the parameter values, and the simulations of the model. Finally, in chapter 5 we draw our conclusions and outlook.

Chapter 2

Theory

In this chapter theory that applies to this thesis will be covered. We start by explaining the basic principles behind an STM. Next, we will cover superconductivity, what phenomena result from it and why. We will explain what a Josephson junction is, the corresponding Josephson equations and resulting effects. We close the chapter by describing how the STM and the Josephson junction come together in the J-STM.

2.1 Scanning tunneling microscope

An STM is a type of microscope that is able to do measurements of materials at the atomic level [1] by making use of the quantum tunneling phenomenon. Which is the effect in quantum mechanics when a particle, for instance an electron, has a probability to go through a potential barrier while, viewed classically, it does not have enough energy to overcome that barrier [2]. The resulting tunneling current depends on the distance of separation. By bringing a very sharp conducting tip, of only one atom thickness, close to a conducting sample, and applying a bias voltage, electrons will start to tunnel through the vacuum barrier separating the tip and the sample. The schematics of an STM are shown in figure 2.1. As the tunneling current depends on the distance of separation it is for instance a way to map out the surface of the sample. But this is not the only application. There is for instance also spectroscopic-imaging, which measures the number of electrons as a function of the electron energy. When we build the STM with, instead of normal conducting elements, superconducting elements, interesting things happen.

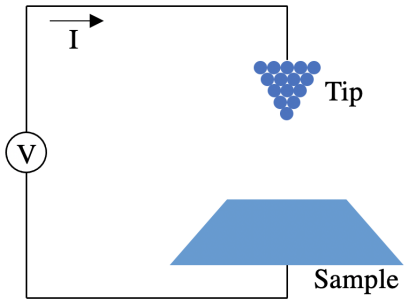

Figure 2.1: *Schematics of a Josephson STM.*

2.2 Superconductivity

To explain the concept of superconductivity, we start by explaining normal conductivity. Electrical current in a normal conductor is like a fluid of single electrons flowing through a lattice of ions. By flowing through the lattice, the electrons constantly collide with the ions and transform little of its kinetic energy into heating of the lattice. The energy is constantly dissipating, known as electrical resistance. In 1911, Kamerlingh Onnes discovered that some materials, when cooled below the critical temperature T_c, suddenly started to show interesting behaviour [3]. The electrical resistance completely disappeared. For instance, giving rise to persistent currents in a superconducting wire that can run indefinitely without a power source, *perfect conductivity*. In 1933, Meissner and Ochsenfeld discovered that a magnetic field in an originally normal conducting material is expelled as it is cooled below T_c, *perfect diamagnetism* [3, 4]. We call these materials superconductors. In a superconductor, electrons can overcome their usual repulsion by interaction with phonons and pair up to form so called Cooper pairs [5]. Electrons have half-integer spin, and so they are fermions. But the total spin of Cooper pairs is integer, which makes it a composite boson. Hence, the wave function is symmetric under particle interchange. And allows the Cooper pairs, unlike single electrons, to be in the same quantum state. When the superconductor is cooled below T_c, the Cooper pairs establish phase coherence and macroscopically condense into the same quantum state with phase ϕ, the superfluid. In a superconductor the fluid consists of Cooper pairs. These Cooper pairs have a certain binding energy gap Δ. Now, if this energy gap is larger than the thermal energy of the lattice kT (with k the Boltzmann constant and T the temperature), the Cooper pair fluid will not be scattered by the lattice. Unlike in a normal conductor, it will flow through the lattice without dissipation and zero resistivity, a superfluid.

Version of February 15, 2022– Created February 15, 2022 - 12:59

2.3 The Josephson junction

In 1962, Josephson predicted that when we bring two superconducting materials very close together separated by something non-superconducting (figure 2.2), a current should start to flow [6]. This type of current is called a supercurrent, consisting of Cooper pairs that flow without any applied voltage. Before then, it was only known that single electrons could tunnel through insulating barriers. The superconducting parts A and B in figure 2.2 are assumed to have Ginzburg-Landau order parameter of the form: $\psi_A = \sqrt{n_A}e^{i\phi_A}$ and $\psi_B = \sqrt{n_B}e^{i\phi_B}$ [7]. Where the superconducting parts A and B have superfluid densities n_A and n_B, respectively. These order parameters may be viewed as the wave functions of the Cooper pairs. Then, using the laws of quantum mechanics, the first and second Josephson relations, equations 2.1 and 2.2, can be deduced.

$$I_s = I_c \sin\varphi \tag{2.1}$$

$$\frac{\partial\varphi}{\partial t} = \frac{2eV}{\hbar} \tag{2.2}$$

Where, I_s is the supercurrent, I_c the critical current, V the voltage, e the unit of electric charge and $\hbar$ the reduced Planck's constant. The Josephson phase φ is the phase difference of Ginzburg-Landau order parameters. So, $\varphi = \phi_B - \phi_A$.

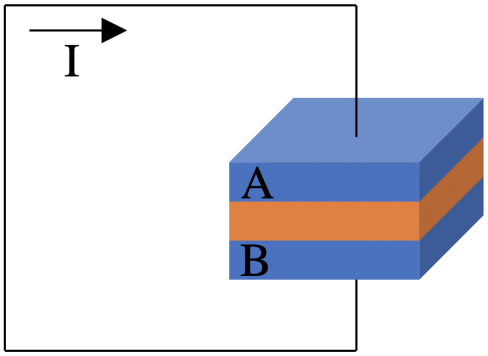

Figure 2.2: *Schematics of a Josephson junction. With the two superconducting parts A and B, which are separated by something non-superconducting.*

2.3.1 DC Josephson effect

When no voltage is applied across the junction, the Josephson phase φ stays constant over time (equation 2.2). Now, because the supercurrent is proportional to

the sine of φ (equation 2.1), the supercurrent will be a direct current taking a value between $-I_c$ and I_c, depending on $\sin\varphi$. Called the direct current (DC) Josephson effect.

2.3.2 AC Josephson effect

From equation 2.2 we see that when applying a voltage, the Josephson phase φ will vary linearly over time, and the resulting supercurrent will thus be an oscillating current of amplitude I_c. We call this the alternating current (AC) Josephson effect. As a fixed voltage results in a perfect alternating current, the Josephson junction can be used as a voltage-to-frequency converter.

2.4 Josephson STM (J-STM)

When we make the tip and the sample of the STM of superconducting materials, we do not have our usual STM anymore. The tip-sample system can now be considered an ultra-small Josephson junction of one atom thickness and we have a J-STM (see figure 2.3). The equations and effects described in section 2.3 are now valid for our system. As we will discover in chapter 3, some of the frequency dependent effects in the J-STM are related to the superfluid densities, n_t and n_s, of the tip and sample. We combine the knowledge and experience in the field of the STM present at the Allan Lab, with the effects and equations that describe the Josephson junction to produce new methods that will allow us to determine the superfluid density of superconductors.

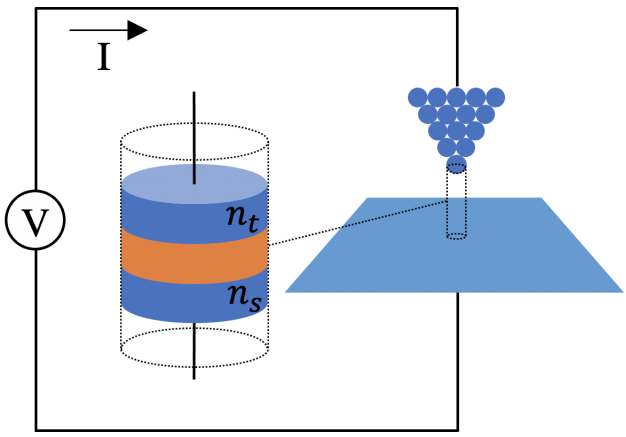

Figure 2.3: *Schematics of a Josephson STM. The superconducting tip and sample have superfluid density n_t and n_s, respectively.*

Chapter 3

Frequency dependent physical quantities in a J-STM that are related to the superfluid density n

The main aim of this research is to present a method that will allow us to determine the superfluid density n of superconductors by using a J-STM. In this chapter we discuss the frequency dependent physical quantities that arise from the J-STM and are related to the superfluid densities of the superconducting tip and sample. And with that, discover routes that may lead to the ability to calculate n_t and n_s. We explain how the J-STM gives rise to the frequency dependent kinetic inductance L_k and Josephson inductance $L_J(\varphi)$ and how these quantities relate to the superfluid densities of the tip and the sample.

3.1 Kinetic inductance L_k

Kinetic inductance L_k is a frequency dependent material-property in superconductors that arises from the Drude model and originates from the kinetic energy of the moving charge carriers [8]. Charged particles in electromagnetic fields experience an electromagnetic force, the Lorentz force, which causes an acceleration. Like all objects, the charged particles prefer to travel at constant velocity. The force is opposed by the inertia of the particle. And so it takes time to accelerate a particle and convert the Lorentz force that is applied into motion. Hence, when the electromagnetic fields alternate, kinetic inductance manifests itself just like a regular inductance. L_k depends on material properties of the superconductor as well as the size and dimensionality of the superconductor. For a Josephson junction we have a contribution to the total kinetic inductance from both the tip and the sample. We

compared three methods described in literature to calculate L_k for various systems and chose which method suits our system best. First of all, for a Josephson junction in an ultra-cold 2D homogeneous Fermi gas, the kinetic inductance is given by equation 3.1 [9].

$$L_k = \frac{8m}{\pi^2 n} \cdot \frac{l_\perp}{l_\parallel} \tag{3.1}$$

Where, $l_\perp$ and $l_\parallel$ are the length and width of the junction. Since, in their research, both superconducting parts are of the same material and size and because the separating barrier is very small relative to the junction, the whole junction is approached as one bulk. It differs from a J-STM as we need to calculate L_k for the tip and sample separately and add those. In 1969, [10] found that for the kinetic inductance of long thin wires with length l and very small cross-sectional area σ, the material enters by a factor $\Lambda = \frac{m}{ne^2}$ and the geometry enters by a factor l/σ (equation 3.2).

$$L_k = \frac{m}{ne^2} \cdot \frac{l}{\sigma} \tag{3.2}$$

We notice that both, expressions 3.1 and 3.2, have the same structure. A dimensionality scaling factor times m/n, times a geometry factor. Lastly, [11] covers the kinetic inductance specifically for the sample of an STM, equation 3.3.

$$Z_k = i\omega L_k = i\omega\mu_0 \frac{\lambda_{sc}^2}{D} \tag{3.3}$$

With, λ_{sc} the magnetic penetration depth and D the diameter of the tip. In this research D is estimated to be $\sim$ 0.5nm. Since we are interested in the kinetic inductance for a J-STM specifically, equation 3.3 seems best to estimate L_k of the sample. In order to do so we need to find λ_{sc}. From the London formula we know that:

$$\lambda_{sc} = \left(\frac{m^*}{n\mu_0 e^2}\right)^{1/2} \tag{3.4}$$

Where, m^* is the effective mass. Since, L_k depends on λ_{sc}, which depends on n_s, measuring L_k could lead to the ability to calculate n_s. We now know how to calculate L_k for the sample of the superconductor. But the expression for the tip has not been determined. Equations 3.1 and 3.2 don't seem to correctly describe the kinetic inductance of something that will only be a couple of atoms thick, like the tip of a J-STM. As we did not find a good expression for kinetic inductance of the tip, we only considered the kinetic inductance of the sample.

Version of February 15, 2022– Created February 15, 2022 - 12:59

3.2 Josephson inductance $L_J(\varphi)$

Next to the kinetic inductance, which is a material-property, there is another frequency dependent junction-property in a J-STM, the Josephson inductance. When the supercurrent and the Josephson phase φ vary over time, the voltage will also vary over time. Looking at the first and second Josephson equations, equation 2.1 and 2.2, and rearranging a bit, yields the Josephson inductance [12]. We start by taking the first time-derivative of the first Josephson equation:

$$\frac{dI_s}{dt} = \frac{d}{dt}\Big[I_c \sin\varphi\Big] = I_c \cos\varphi \frac{d\varphi}{dt}$$

Substituting the second Josephson equation into the equation above, we get:

$$\frac{dI_s}{dt} = I_c \cos\varphi \cdot \frac{2eV}{\hbar}$$

Now, inductance L is defined as the ratio between the voltage and the time derivative of the current, $V = L \cdot \frac{dI}{dt}$. Hence, we can define another kinetic inductance $L_J(\varphi)$:

$$L_J(\varphi) \equiv \frac{\hbar}{I_c \cos\varphi \cdot 2e} = \frac{L_{J,0}}{\cos\varphi} \tag{3.5}$$

$$L_{J,0} \equiv \frac{\hbar}{2eI_c} \tag{3.6}$$

As we can see in equation 3.5, $L_J(\varphi)$ depends on the phase difference φ and the critical current I_c. For a Josephson STM, the relation of the critical current I_c to the superfluid densities of the tip and the sample is given by D. Cho et al. [13]:

$$I_c = \kappa \sqrt{n_t}\sqrt{n_s} \tag{3.7}$$

Where, n_t and n_s correspond to the superfluid densities of the tip and the sample. And κ is a coupling constant. So, for a junction consisting of two different superconductors, if we know κ and n_B, measuring the critical current I_c would allow us to calculate n_A. For a junction where the two parts are of the same superconductor (in which case, $n_A = n_B = n$), the situation becomes even simpler. If we know κ and measure I_c we can calculate n. Thus, in the case that we know φ, measuring $L_J(\varphi)$ allows us to calculate I_c and therefore n. However, that might be easier said than done. In equation 3.5, $1/\cos\varphi$ has asymptotes at $\varphi = \frac{\pi}{2} \pm m \cdot \pi$ with $m = 1, 2, 3, \ldots$. Therefore, $L_J(\varphi)$ will also show asymptotic behaviour as shown in figure 3.1. In the discussion (chapter 5), we elaborate on this matter.

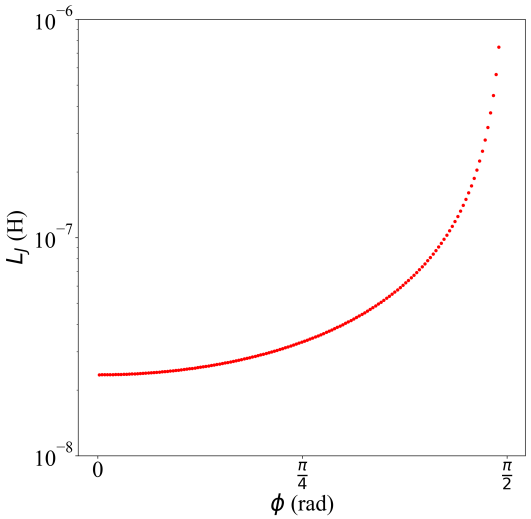

Figure 3.1: *Josephson inductance $L_J(I_c$=14nm,$\varphi)$ is plotted for the range φ=(0,$\pi/2$) to show the asymptotic behaviour.*

Chapter 4

Results

In chapter 3 we described how certain frequency dependent physical quantities in a J-STM are related to the superfluid densities of the tip and the sample. Still those physical quantities need to be measurable. In this chapter we show how that can be achieved. We start by presenting the electrical circuit that we used to model the J-STM and explain what parameters are present in this circuit. We derive the corresponding equation for the total impedance and the resonance frequency. We simulate the system with arbitrary parameters and analyze the behaviour of our model. Finally, we estimate the parameters for a J-STM, simulate it again and explain how we are able to deduce the superfluid densities of the tip and the sample.

4.1 The LC circuit model

To measure properties of a J-STM, the system needs to be modeled as an electrical circuit. Next, it needs to be determined how to relate, for instance a resonance frequency or a supercurrent, to the parameters of such a model. There is not just a single model. Mostly because a Josephson junction shows different behaviour for different types of input. One of such inputs is high frequency. This research investigates the high frequency properties of a Josephson junction.

4.1.1 Circuit

Since we are only interested in the frequency dependent behaviour of a Josephson junction, some models not suit anymore. At high frequency, when the current and phase vary over time, there is no supercurrent anymore. In chapter 3 we learned that a varying current and phase yields a Josephson inductance. N. Luick at al. [9]

imprinted a relative phase between two sides of a Josephson junction, and from it extracted the population imbalance and phase. The current and phase oscillate and so the frequency dependent properties of the junction are of importance. They modeled the junction as shown in figure 4.1. Which is also the model that we used in this research. The Josephson junction contains three frequency-dependent elements [9]. A capacitive component C, a kinetic inductance L_k and the phase-dependent Josephson inductance $L_J(\varphi)$. The schematics are shown in figure 4.1. As mentioned in section 3.1, this research only considers the kinetic inductance of the sample.

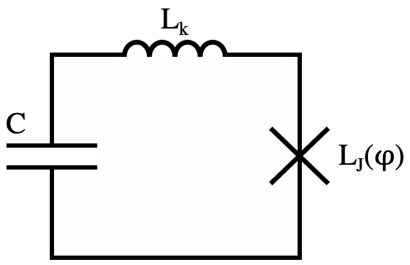

Figure 4.1: *LC circuit model - Electronic circuit representation of the frequency dependent elements of a Josephson junction. With a capacitor C, a kinetic inductance L_k and a Josephson inductance $L_J(\varphi)$.*

4.1.2 The total impedance Z_{tot} and the resonance frequency ω_c

To find the resonance frequency of this system we first write down the total impedance Z_{tot} of the system. For which we need to know how the impedance of the capacitive and inductive components depend on frequency. For capacitors and inductors we have $Z_C = \frac{1}{i\omega C}$ and $Z_L = i\omega L$, respectively. According to Kirchhoff's laws, the total impedance of components added in series is given by the sum of all components. Hence, the total impedance of our model is:

$$Z_{tot} = Z_C + Z_{L_k} + Z_{L_J} = \frac{1}{i\omega C} + i\omega L_k + i\omega L_J(\varphi) \tag{4.1}$$

Now, we get a resonance if the imaginary part of the total impedance equals zero.

Version of February 15, 2022– Created February 15, 2022 - 12:59

$$\mathrm{Im}\{Z_{tot}\} = 0$$

$$\frac{1}{\omega C} + \omega L_k + \omega L_J(\varphi) = 0$$

$$\Rightarrow \quad \omega_c = \sqrt{\frac{1}{(L_k + L_J(\varphi))C}} \tag{4.2}$$

As mentioned in subsection 3.2, to our understanding $L_J(\varphi)$ shows asymptotic behaviour. For our simulations we assumed the phase to be the same as in subsection 4.2.3. Simulation of the total impedance of our model (equation 4.1) with arbitrary values for C, L_k and $L_J(\varphi)$ is shown in figure 4.2.

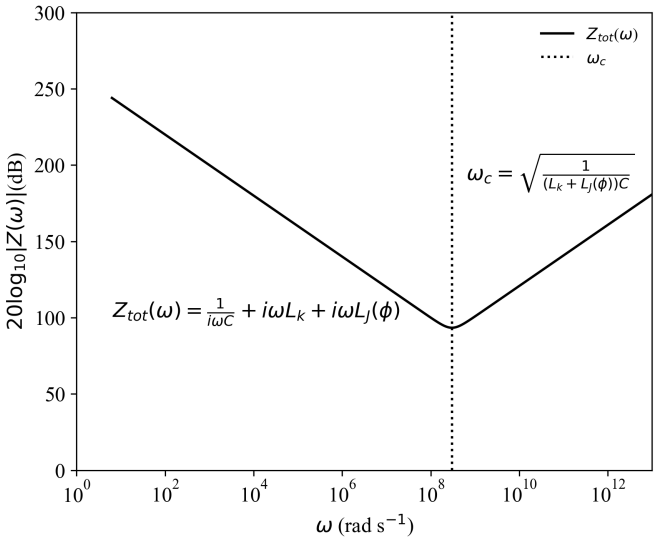

Figure 4.2: *Simulation of LC circuit model. Arbitrary parameters have been inserted to look at the characteristics of equation 4.1; $C = 10^{-13}F$, $L_k = 10^{-5}H$ and $L_J(\varphi) = 10^{-4}H$. The behaviour of the curve is as expected when we analyse equation 4.1. C and L_k are, by definition, greater then zero. Thus, we expect, on a logarithmic scale, the capacitance giving a negative linear contribution to the impedance. Because $\frac{1}{i} = -i$. And two positive linear contributions on a logarithmic scale, that of L_k and $L_J(\varphi)$. Also, the resonance frequency agrees with the one obtained from equation 4.2.*

4.2 Finding parameter values

In chapter 3 we learned that measuring the kinetic inductance L_k or Josephson inductance $L_J(\varphi)$, means being able to calculate the superfluid densities of the tip and the sample, n_t and n_s. From equation 4.2 we know that the resonance frequency depends on those two physical quantities. Therefore, we want to determine what the curve would look like for a real J-STM, how it behaves when changing the individual parameters and whether the resonance lies below 1 THz (measurable range for the Allan Lab). Because then we can determine whether it is a possibility that measuring ω_c allows calculating L_k or $L_J(\varphi)$, which would mean that we can calculate n_t and n_s. In this section we investigate what values the parameters would take on for a J-STM.

4.2.1 Capacitance C

The first parameter that we will estimate the range for, in a J-STM, is the tip-sample capacitance. Three different papers show different orders of magnitude for the tip-sample capacitance in an STM.

J.M. De Voogd et al.[14] analyzed several completely different systems, and found that the absolute tip-sample capacitance shows generic behaviour as a function of the distance. All measurements showed capacitances of the order of magnitude $\sim 1 - 4 \cdot 10^{-13}$F. Other research, that of D. Cho et al.[13] estimated for an STM the tip-sample capacitance to be $\sim 1 \cdot 10^{-15}$F. Finally, S. Kurokawa et al.[15] measured the tip-sample capacitance on multiple tips with different radius ranging from 30 nm to 2100 nm. Mostly measurements with C $\sim 1 - 5 \cdot 10^{-16}$ F, but also around $\sim 1 \cdot 10^{-17}$ F.

To conclude, in the literature we found that the tip-sample capacitance, varies greatly with values ranging from 10^{-17}F to 10^{-13}F. Because it varies so greatly, we took an even wider range (one order of magnitude smaller and bigger) to put in our final simulations. Namely a range of 10^{-18}F up to 10^{-12}F.

4.2.2 Kinetic Inductance L_k

Using previous published experimental data [16] of the superfluid density n of multiple superconductors, we can calculate λ_{sc} with equation 3.4 and thereby estimate L_k using equation 3.3, following the method described in section 3.1. The published data, λ_{sc} and L_k are presented in table 4.1. We obtained estimates for L_k mostly around $\sim 10^{-12}$H. Only for Nb-doped STO L_k was estimated to be $\sim 2.60 \cdot 10^{-9}$H.

Version of February 15, 2022– Created February 15, 2022 - 12:59

Sample	n (10^{28} m^{-3})	m^*/m_e	λ_{sc} (nm)	L_k (H)
Sn	14.8	1.26	$1.55{\cdot}10^{-8}$	$6.04{\cdot}10^{-13}$
Pb	13.2	1.97	$2.05{\cdot}10^{-8}$	$1.05{\cdot}10^{-12}$
Nb (15.3nm)	5.56	1.81	$3.03{\cdot}10^{-8}$	$2.31{\cdot}10^{-12}$
NbN-1	16.85	1.0	$1.30{\cdot}10^{-8}$	$4.21{\cdot}10^{-13}$
MoGe-1 (21nm)	46	1.0	$7.84{\cdot}10^{-9}$	$1.55{\cdot}10^{-13}$
Nb-doped STO	0.011	4.0	$1.01{\cdot}10^{-6}$	$2.60{\cdot}10^{-9}$

Table 4.1: *For different superconductors the superfluid density n and m^*/m_e were extracted from [16]. Then, using equation 3.4, the magnetic penetration depth λ_{sc} of the superconductor was calculated after which the kinetic inductance L_k was calculated using equation 3.3.*

4.2.3 Josephson Inductance $L_J(\varphi)$

First of all, N. Luick at al. [9] calculated $L_{J,0}/\hbar$, for a homogeneous 2D Fermi gas of Li^6 atoms, to be within a range of $\sim 20-40$ μs. Dimensional analyses shows that the charge of the carriers is left out in the paper. And so, when divided by $(2e)^2$ the square of the charge of the carriers and multiplied by $\hbar$ we get a range for $L_{J,0}$ of $\sim 8-16\cdot10^{-8}$H or roughly $\sim 10^{-7}$H. In their research they assumed small phase oscillations such that $L_J(\varphi)$ can be approximated by a time-independent Josephson inductance $L_{J,0}$. We are interested in an ultra-small tip-sample junction, not a regular junction. Nevertheless, it does give somewhat of an indication of the order of magnitude to think of when estimating $L_J(\varphi)$.

Secondly, $L_J(\varphi)$ was estimated for a specific phase using published data of the critical current I_c from K. Bastiaans et al. [17]. Who measured the supercurrent I_s in a Pb-Pb J-STM, exactly in line with what this research is about. From the I_s measurement, the critical current I_c was calculated using the Ambegaokar-Baratoff formula. Their data is shown in figure 4.3. Recall the first Josephson relation and the equation for the Josephson inductance, equations 2.1 and 3.5:

$$\varphi = \arcsin\left(\frac{I_s}{I_c}\right) \tag{2.1}$$

$$L_J(\varphi) = \frac{\hbar}{I_c\cos\varphi\cdot 2e} \tag{3.6}$$

Now, using the measurements of I_s and I_c from K. Bastiaans et al. [17], we can calculate φ using equation 2.1 and L_J using equation 3.6.

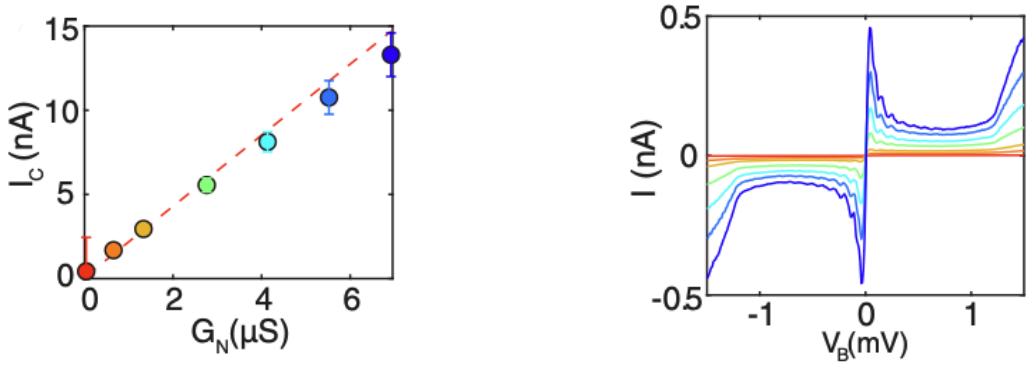

Figure 4.3: *Measurements from K.M. Bastiaans et al. [17]. On the left and right we see the I_c and I_s, respectively.*

Since we are only interested in the order of magnitude of the parameters, the exact value is not very important, and so estimating I_c and I_s from figure 4.3 by eye is enough. We chose to estimate the blue curve, as it is easiest to accurately estimate it by eye. Nevertheless, calculating L_J with estimated values of the other curves gives the same order of magnitude. We estimated for the blue curve $I_c \approx 14$ nA and $I_s \approx 0.45$ nA. Then, using equation 2.1 we calculated $\varphi \approx 0.032$ and with equation 3.6, $L_J(\varphi = 0.032) \approx 2.4 \cdot 10^{-8}$H. In table 4.2 we present the ranges that we found for all three parameters C, L_k and $L_J(\varphi = 0.032)$

Parameter	order of magnitude range
C	$(10^{-18} - 10^{-12})$F
L_k	$(10^{-13} - 10^{-9})$H
$L_J(\varphi = 0.032)$	$(2.4 - 16)10^{-8}$H

Table 4.2: *Final order of magnitude ranges for the three parameters C, L_k and $L_J(\varphi = 0.032)$ of equation 4.1*

.

4.3 Simulation

Now that we estimated the order of magnitude for all three parameters (C, L_k and $L_J(\varphi = 0.032)$) of equation 4.1, we are able to simulate how a real J-STM would

behave and look whether the resonance will lie below the measurable limit of 1 THz lie. First of all, we investigated how the total impedance Z_{tot} and resonance frequency ω_c change when varying the capacitance C and kinetic inductance L_k while keeping $L_J(\varphi = 0.032)$ constant at $2.4 \cdot 10^{-8}$H. See figure 4.4.

Analyzing equation 4.2, reveals that when either L_k or $L_J(\varphi)$ is significantly higher in order of magnitude than the other one, the resonance frequency ω_c is only sensitive to that parameter. Since, both L_k and L_J depend on the superfluid densities n_t and n_s, both cases $L_k \gg L_J$ and $L_k \ll L_J$ are good to determine the superfluid densities. In the case that L_k and $L_J(\varphi)$ are of the same order of magnitude, in order to determine one of the two parameters, the other one must be known. As it stands, it looks like for a J-STM $L_k \ll L_J$ and so the resonance is sensitive to $L_J(\varphi)$ and not L_k. Next, we looked at what happens when we vary L_J, keeping L_k constant at 10^{-9}H. We could have equally well chosen the other limit of 10^{-13}H, since we already found it has negligible impact on the curve. See figure 4.5.

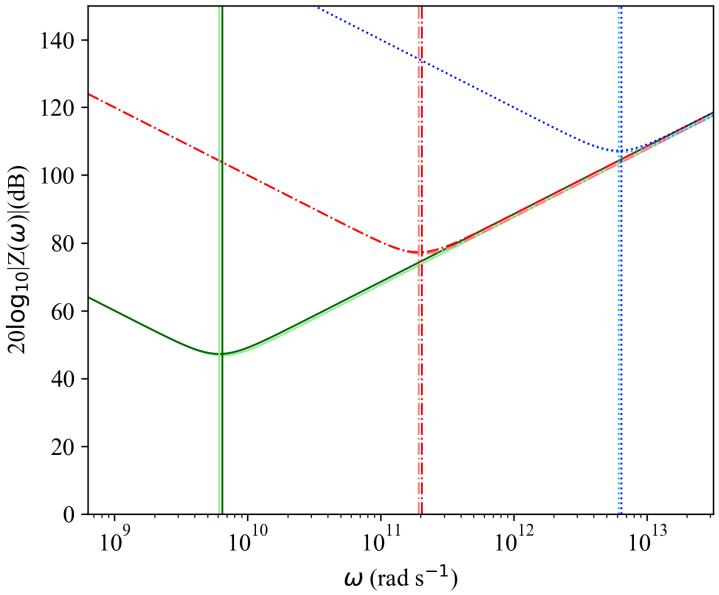

Figure 4.4: *Simulation of the LC circuit model. Real parameters have been inserted to simulate the frequency dependent properties of a Josephson STM. $L_J(\varphi = 0.032)$ is kept constant at $2.4 \cdot 10^{-8}H$, while C and L_k change. The greenish/solid curves correspond to $C = 10^{-12}F$, the reddish/dashdotted curves correspond to $C = 10^{-15}F$ and the blueish/dotted curves correspond to $C = 10^{-18}F$. Then, for each value of C, we plotted two curves. One with $L_k = 10^{-9}H$ (light curves), the upper limit of L_k that we found. And one with $L_k = 10^{-13}H$ (dark curves), the lower limit of L_k that we found. It is almost impossible to separate the two curves from each other. The curves lie on top of each other even though the difference is 4 orders of magnitude. Even the little shift caused by a change of 4 orders in magnitude is rare, as all materials that we calculated L_k for, expect Nb-doped STO, had $L_k \sim 10^{-12} - 10^{-13}$. When we analyze equation 4.2 it becomes clear why. C is multiplied by the sum of L_k and $L_J(\varphi)$, hence the parameter (L_k or $L_J(\varphi)$), that has a significantly lower order of magnitude than the other is negligible in terms of the product $C(L_k + L_J(\varphi))$, and therefore where the resonance ω_c lies. Since, $L_J(\varphi = 0.032)$ is of order of magnitude $10^{-8}H$, we expect that varying L_k between $10^{-13}H$ and $10^{-9}H$ will have a negligible effect on the resonance, which agrees with what we see in this figure. We also notice that the blueish curves, that correspond to $C = 10^{-18}F$, lie outside of the measurable range.*

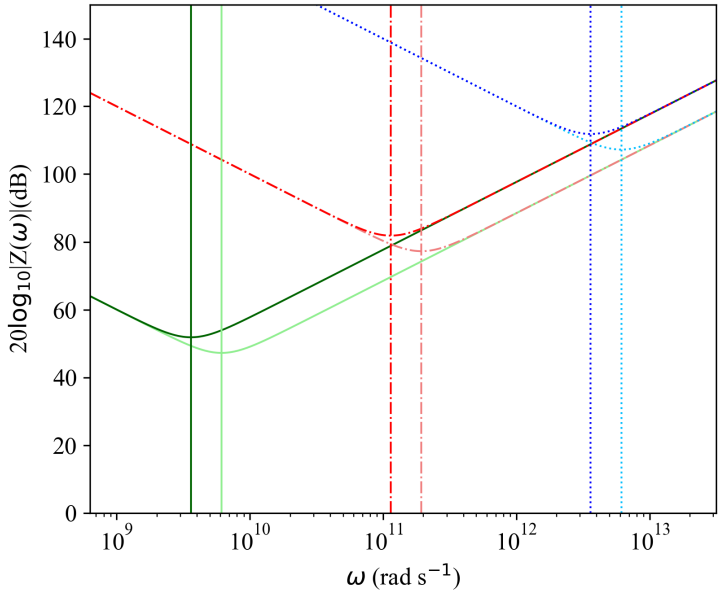

Figure 4.5: *Simulation of the LC circuit model. Again, real parameters have been inserted to simulate the frequency dependent properties of a Josephson STM. Again, the greenish/solid curves correspond to* $C = 10^{-12}F$*, the reddish/dashdotted curves correspond to* $C = 10^{-15}F$ *and the blueish/dotted curves correspond to* $C = 10^{-18}F$*. However this time,* L_k *is kept constant at* $10^{-9}H$*. For each value of* C *we plotted one curve with* $L_J(\varphi = 0.032) = 2.4 \cdot 10^{-8}H$ *(light curves), and one curve with* $L_J(\varphi = 0.032) = 7.4 \cdot 10^{-8}H$ *(dark curves). We see that changing* $L_J(\varphi = 0.032)$ *by only half an order of magnitude clearly shifts the resonance frequency. Just as we expected. We also notice that the blueish curves, that correspond to* $C = 10^{-18}F$*, lie outside of the measurable range*

Chapter 5

Conclusion and Discussion

The Josephson STM (J-STM) gives rise to the frequency dependent kinetic inductance and Josephson inductance. Which are physical quantities that are related to the superfluid densities of the tip and the sample, n_t and n_s, respectively. So, determining L_k or $L_J(\varphi)$ means ability to calculate n_t and n_s. We can represent the frequency dependent properties of the J-STM as an electrical circuit containing a capacitor C, kinetic inductor L_k and Josephson inductor $L_J(\varphi)$ connected in series, the LC circuit. This circuit has a certain total impedance (eq. 4.1) and resonance frequency ω_c (eq. 4.2) that depend upon those three parameters. When either L_k or $L_J(\varphi)$ is significantly higher in order of magnitude than the other one, ω_c is only sensitive to that parameter. Since, both L_k and L_J depend on n_t and n_s, both cases $L_k \gg L_J$ and $L_k \ll L_J$ are good to determine n_t and n_s. In the case that L_k and $L_J(\varphi)$ are of the same order of magnitude, in order to determine one of the two parameters, the other one must be known. As it stands, it looks like for a J-STM $L_k \ll L_J$ and so the resonance is sensitive to $L_J(\varphi)$ and not L_k. Thus, in the case that we know C very precisely, which is certainly not a given (but maybe possible with feedback control), we can determine $L_J(\varphi)$ through measuring ω_c. Then, from $L_J(\varphi)$, if we know φ, we can deduce the critical current I_c. And with that, n_t and n_s. All provided that ω_c lies below 1 THz, which it probably does.

We found that the value of the tip-sample capacitance C in an STM highly depends on the separation distance. In the literature we found values ranging between 10^{-13}F and 10^{-17}F. However, the values are found for many different types of systems and different materials. The outer boundary of around $C = 10^{-17} - 10^{-18}$F resulted in a resonance frequency ω_c higher than the measurable limit (1THz). But mostly, the capacitances that we found were much bigger and resulted in ω_c being measurable.

The kinetic inductance L_k will have a contribution from the tip and from the sample. The expression for the tip was not found and we only considered L_k of the sample. L_k of the sample was calculated for different superconductors and ranged between 10^{-9}H and 10^{-13}H.

Finally, the Josephson inductance $L_J(\varphi)$, for 2 different systems, was found to be of the order of magnitude $\sim 10^{-8} - 10^{-7}$H. As mentioned in subsection 3.2, $L_J(\varphi)$ shows asymptotic behaviour. This means that for $\varphi = \frac{\pi}{2}$, L_J would go to plus or minus infinity. Which is strange. And for which we don't have a physical explanation. If given more time we would try to investigate this matter. In figure 5.1 we show what kind of influence the phase-dependence of L_J has on the curve and ω_c. It looks like that for certain curve, there are endless possibilities in terms of which combination of I_c and φ resulted in that curve.

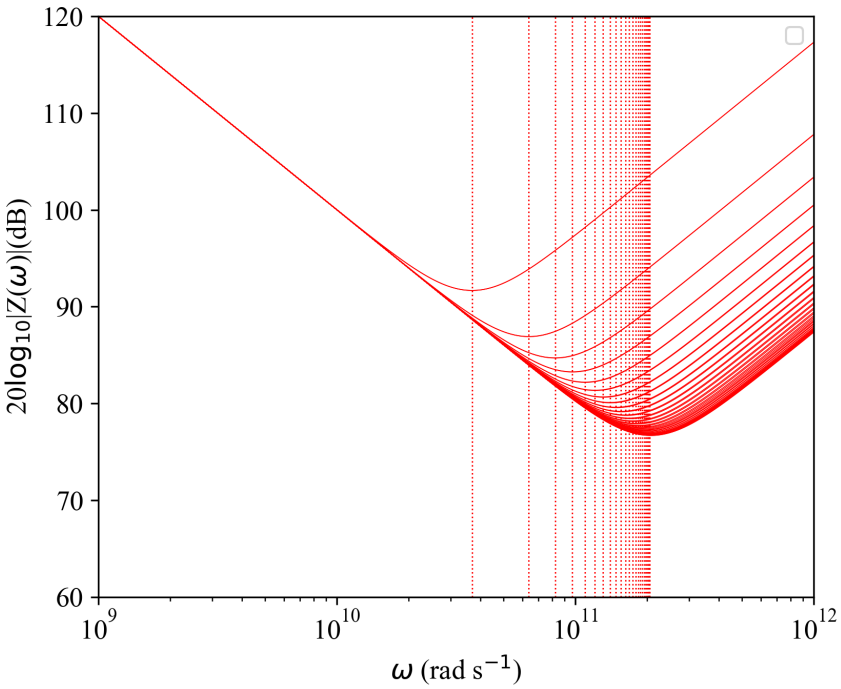

Figure 5.1: *Simulation of the LC circuit - Here we simulated the system for $C = 10^{-15}F$ and $L_k = 10^{-14}H$. But this time we calculated $L_J(\varphi, I_c{=}14)$ with $\varphi = (\frac{\pi}{2}, \pi)$. When we compare this figure with figure 3.1, we notice that the 'tail' of the asymptote in figure 3.1, corresponds to the left side of the bunch of curves. The 'belly' of the curve in figure 3.1, corresponds to the right side of the bunch of curves.*

If given more time we would continue the research by investigating the following things. First of all, the contribution to the kinetic inductance of the tip. Secondly, in order for the method presented in this thesis to work, the capacitance must be known exactly. We would try to investigate whether that is achievable. Also, in this research temperature dependence was left out. But the superfluid density is dependent on the temperature [16], and therefore the method presented in this research also. In addition, during the simulations we noticed that all resonance peaks had different depths. Maybe there is a certain threshold for a resonance to be measurable. Also, equation 3.7, that relates I_c to n_t and n_S has a coupling constant κ that needs to be determined as well. Finally, throughout the research it is assumed that we know how to measure the resonance frequency ω_c, but that is not the case. We think it can be achieved with transmission lines. But also that needs to be investigated.

Bibliography

[1] G. Binnig, H. Rohrer, C. Gerber, and E. Weibel, "Surface studies by scanning tunneling microscopy," *Phys. Rev. Lett.*, vol. 49, pp. 57–61, Jul 1982.

[2] J. Tersoff and D. R. Hamann, "Theory of the scanning tunneling microscope," *PHYSICAL REVIEW B*, vol. 31, 1985.

[3] M. Tinkham, *Introduction to Superconductivity*. Dover Publications, pages 1-19, 1996.

[4] A. Forrest, "Meissner and ochsenfeld revisited," *European Journal of Physics*, vol. 4, p. 117, 12 2000.

[5] L. N. Cooper, "Bound electron pairs in a degenerate fermi gas," *physical review*, vol. 104, no. 4, 1956.

[6] B. D. Josephson, "Possible new effects in superconductive tunnelling," *Physics Letters 1*, vol. 1, no. 7, 1962.

[7] R. Feynman, "The feynman lectures on physics vol. iii ch. 21: The schrödinger equation in a classical context: A seminar on superconductivity, section 21-9: The josephson junction," *Physics*, vol. 3, Ch. 21.

[8] W. C. J. J. Kunjesh Agashiwala, Arnab Pal and K. Banerjee, "Can Kinetic Inductance in Low-Dimensional Materials Enable a New Generation of RF-Electronics?," *Technical Digest - International Electron Devices Meeting, IEDM*, vol. 2018-December, no. December, pp. 24.4.1–24.4.4, 2019.

[9] N. Luick, L. Sobirey, M. Bohlen, V. P. Singh, L. Mathey, T. Lompe, and H. Moritz, "An ideal josephson junction in an ultracold two-dimensional fermi gas," Aug 2019.

[10] R. Meservey and P. M. Tedrow, "Measurements of the kinetic inductance of superconducting linear structures," *Journal of Applied Physics*, vol. 40, pp. 2028–2034, 1969.

[11] S. Kalinin et al., *Scanning Probe Microscopy (page 228)*. Springer, 2007.

[12] M. H. Devoret, A. Wallraff, and J. M. Martinis, "Superconducting Qubits: A Short Review," 2004.

[13] D. Cho, K. M. Bastiaans, D. Chatzopoulos, G. D. Gu, and M. P. Allan, "A strongly inhomogeneous superfluid in an iron-based superconductor," *Nature*, vol. 571, pp. 541–545, Jul 2019.

[14] J. M. de Voogd, M. A. van Spronsen, F. E. Kalff, B. Bryant, O. OstojiÄ, A. M. den Haan, I. M. Groot, T. H. Oosterkamp, A. F. Otte, and M. J. Rost, "Fast and reliable pre-approach for scanning probe microscopes based on tip-sample capacitance," *Ultramicroscopy*, vol. 181, pp. 61–69, Oct 2017.

[15] S. Kurokawa et al., "Tip-sample capacitance in stm(stm-beem interfaces)," 1997.

[16] S. Dutta, P. Raychaudhuri, S. S. Mandal, and T. V. Ramakrishnan, "Superfluid density in conventional superconductors: From clean to strongly disordered," Jan 2021.

[17] K. M. Bastiaans, D. Cho, D. Chatzopoulos, M. Leeuwenhoek, C. Koks, and M. P. Allan, "Imaging doubled shot noise in a josephson scanning tunneling microscope," *Phys. Rev. B*, vol. 100, p. 104506, Sep 2019.